A New Source of Basaltic Meteorites Inferred from Northwest Africa 011

Akira Yamaguchi,[1,2]* Robert N. Clayton,[3] Toshiko K. Mayeda,[3] Mitsuru Ebihara,[4] Yasuji Oura,[4] Yayoi N. Miura,[5] Hiroshi Haramura,[1] Keiji Misawa,[1,2] Hideyasu Kojima,[1,2] Keisuke Nagao[6]

Eucrites are a class of basaltic meteorites that share common mineralogical, isotopic, and chemical properties and are thought to have been derived from the same parent body, possibly asteroid 4 Vesta. The texture, mineralogy, and noble gas data of the recently recovered meteorite, Northwest Africa (NWA) 011, are similar to those of basaltic eucrites. However, the oxygen isotopic composition of NWA011 is different from that of other eucrites, indicating that NWA011 may be derived from a different parent body. The presence of basaltic meteorites with variable oxygen isotopic composition suggests the occurrence of multiple basaltic meteorite parent bodies, perhaps similar to 4 Vesta, in the early solar system.

The diversity of chemical compositions of magmatic iron meteorites indicates the presence of many differentiated planetesimals that were later disrupted (*1*). These bodies may have had a crust composed of basaltic rocks on their surfaces immediately after differentiation but before disruption. However, in our meteorite collections, eucrites are the only abundant basalts [e.g., (*2*)]. Other less abundant asteroidal basalts include angrites and basaltic inclusions in mesosiderites (*2, 3*). Only eucrites can be related with reasonable certainty to a specific asteroid, 4 Vesta, because it shows a basaltic reflection spectrum (*4*). However, it has not been clear whether all eucrites were derived from a single parent body. Here, we report the mineralogy, chemistry, oxygen isotopic compositions and noble gas content of a recently discovered basaltic meteorite, NWA011 (*5, 6*).

The thermal history of NWA011, and some properties of its parent asteroid, may be inferred from its texture and mineralogy. NWA011 is composed of coarse-grained, anhedral clinopyroxene (pigeonite and relict augite) (~1 mm in size) and a fine-grained, granular to stubby (50 to 100 μm in size) plagioclase with well-developed 120° triple junctions and curved boundaries (Fig. 1). There are a few large laths of plagioclase (<0.4 mm by 1.3 mm) which could be relicts of the precursor basalt crystallized rapidly near the surface. This texture indicates that NWA011 is a recrystallized breccia formed by impact event(s). Minor minerals include silica minerals, Ca-phosphate, Ti-rich chromite, ilmenite, Fe-rich olivine, baddeleyite, troilite, and weathering products. In most cases, grains of silica minerals and Ca-phosphate form clusters several mm in size, which are distributed heterogeneously on a scale of a few cm (*7*). Because these minerals generally occur together in mesostasis in basalts as final products of crystallization from the melt, we suggest that they could have been redistributed during high temperature metamorphism (*8*).

The low-Ca pyroxene is pigeonite containing fine exsolution lamellae of augite (less than a few μm thick), similar to equilibrated pyroxenes in type 5 eucrites (type 5 pyroxene) (*9*). The Fe/Mg ratios of low-Ca pyroxene are comparable to those of a eucrite, Lakangaon (*10*). Pairs of pigeonite and augite with the largest Ca difference ($Wo_{39.8}En_{26.4}$ and $Wo_{5.9}En_{32.5}$; where Wo is wollastonite, En is enstatite, and the subscripts indicate molar percentage of the pure endmember phases Wo and En) indicate an equilibration temperature (*11*) of ~860°C. The equilibration temperature (*11*) estimated from the bulk compositions of relict augite and pigeonite ($Wo_{28.2-30.0}En_{26.7-27.6}$ and $Wo_{16.0-16.6}En_{29.5-30.0}$, respectively) is ~1090° to 1110°C, which could represent a peak metamorphic temperature. The FeO/MnO ratios of pyroxene (~65) are higher than those of eucrites (~40) (*12*). The chemical compositions of the fine-grained, granular plagioclase are in the range $Or_{0.3}Ab_{11.0}$to $Or_{0.5}Ab_{22.1}$ (where Or is orthoclase, and Ab is albite). In contrast, the relict plagioclase laths have normal igneous zoning with extensive chemical variations ($Or_{0.2}Ab_{6.1} \sim Or_{1.5}Ab_{35.6}$). Ilmenite is closely associated with Ti-rich chromite, forming a poikiloblastic oxide assemblage. This assemblage may be a decomposition product of ulvöspinel (*13*). In some cases, these oxide assemblages are associated with Fe-rich olivines ($Fa_{81.4-84.5}$ where Fa is fayalite). Some small pyroxenes in contact with the Fe-rich olivines and homogenized type 5 pyroxenes are enriched in Fe ($Wo_{6.1}En_{22.7} \sim Wo_{8.9}En_{25.0}$) compared to the type 5 pyroxenes. The mineralogical features of NWA011 are similar to those of highly metamorphosed eucrites such as EET90020 and Y-86763 (*8, 14*). These facts indicate that NWA011 experienced at least two thermal events, a prolonged thermal metamorphism that produced type 5 pyroxene [e.g., >800° to 1000°C for ~1 million years (Ma)] (*15*) and rapid heating and cooling that produced the oxide-related phases (*8*).

The major and trace element compositions

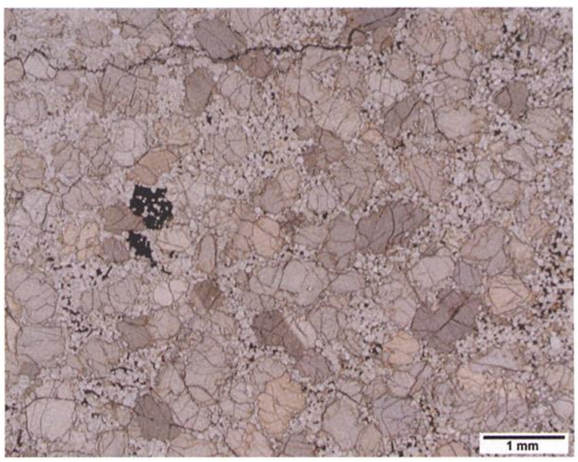

Fig. 1. Photomicrograph of meteorite NWA011. Plane-polarized light. Light brown, pyroxene; fine-grained white, plagioclase; black, opaque minerals (ilmenite, chromite, etc.).

[1]Antarctic Meteorite Research Center, National Institute of Polar Research, Tokyo 173-8515, Japan. [2]The Graduate University for Advanced Studies, Tokyo 173-8515, Japan. [3]Enrico Fermi Institute, University of Chicago, Chicago, IL 60637, USA. [4]Department of Chemistry, Tokyo Metropolitan University, Hachioji, Tokyo 192-0397, Japan. [5]Earthquake Research Institute, University of Tokyo, Tokyo 113-0032, Japan. [6]Laboratory for Earthquake Chemistry, University of Tokyo, Tokyo 113-0033, Japan.

*To whom correspondence should be addressed. E-mail: yamaguch@nipr.ac.jp

of NWA011 (Fig. 2) (*7*) indicate that NWA011 has less SiO_2, P_2O_5, and more FeO and TiO_2 than eucrites (*16*). The FeO/MgO (= 3.17) and CaO/Al_2O_3 (= 0.85) ratios are in the range of eucrites (*16*). We confirmed the high FeO/MnO ratio of ~53 for the bulk sample, consistent with the pyroxene compositions. The heterogeneous distribution of minor minerals such as silica minerals, Fe-rich olivine, and Ca-phosphate observed in NWA011 could have affected the major and trace element abundances. The rare earth element (REE) abundances in our whole-rock sample of NWA011 are two to six times lower than those in typical eucrites, Juvinas and Millbillillie, except for Eu. NWA011 has a fractionated REE pattern, showing a gradual increase from light to heavy REE with a large positive Eu anomaly. The abundances of REE along with a Eu anomaly are not consistent with the previous report (*5*). This is probably due to the heterogeneous distribution of Ca-phosphate, and is consistent with the low abundances of U and Th in our sample (*7*). Compared to eucrites, siderophile elements in NWA011 are highly enriched: Ir in NWA011 is three orders of magnitude higher than Ir in Juvinas and Millbillillie, for which Ir contents are below detection limit, and Co and Ni abundances in NWA011 are about 10 times higher (Fig. 2B). Because the enrichments of siderophile elements cannot be explained in terms of igneous processes, we suggest that NWA011 was contaminated by projectile materials, being consistent with the textural evidence for impact brecciation of NWA011. The high Ni/Ir ratio of NWA011 indicates that the projectile could be IVB iron meteorite-like materials rather than chondritic materials (*17, 18*). Although the bulk compositions were locally disturbed by metamorphism and contamination from the projectile materials, the mineralogical features of NWA011 are similar to those of eucrites.

Cosmic-ray exposure ages, and U-He and K-Ar ages are calculated from the noble gas data (*19*). The most reliable cosmic-ray exposure age for NWA011, determined from cosmogenic ^{21}Ne, is 30 Ma. This age is within the range of the cosmic-ray exposure ages for eucrites, from 7 to 70 Ma (*20*), and is longer than those for martian meteorites ($\lesssim$15 Ma) and lunar meteorites ($\lesssim$11 Ma), and suggests that NWA011 is asteroidal in origin. The concentration of radiogenic ^{40}Ar is 4.5×10^{-6} cm^3/g. This, combined with the bulk K content (*7*), gives a K-Ar age of 2.0 ± 0.3 Ga. Because we cannot exclude the possibility of partial loss of radiogenic ^{40}Ar, the K-Ar age of 2.0 Ga may not represent geologic events on the parent body.

The oxygen isotopic composition of NWA011 ($\delta^{18}O$ = +2.54, $\delta^{17}O$ = −0.48) (*21*) is similar to CR-chondrites, and falls between the terrestrial fractionation (TF) line and the carbonaceous-chondrite anhydrous-mineral mixing (CCAM) line (*22*) (Fig. 3). No other achondrites are found in this region (*23*). The $\Delta^{17}O$ (*21*) of NWA011 is –1.80, in contrast to $\Delta^{17}O$ = −0.25 for eucrites (*23*). This indicates that NWA011 is a new type of basaltic meteorite, with no genetic relationship with to eucrites.

Mineralogical and chemical data indicate that NWA011 is a basalt that formed by extensive melting and differentiation in the parent body. The postcrystallization thermal history of NWA011 can be explained by the burial of basalt, originally crystallized near the surface, under several kilometers of crustal rock in a large asteroid like 4 Vesta (*24*), followed by impact excavation during slow cooling (*8*). The mineralogical similarities between NWA011 and eucrites imply infrared spectral properties similar to 4 Vesta or Vestoids (*4, 25*). It is unlikely that the eucrite parent body is heterogeneous with respect to oxygen isotopes after extensive melting and differentiation. Thus, NWA011 was derived from a parent body that formed from a solar system reservoir different from the eucrite parent body. The observations further suggest that Vesta is not the only source for the basaltic meteorites, consistent with the recent discovery of a large asteroid with a basaltic surface, but no dynamical link to Vesta (*26*). This study shows the evidence for the presence of multiple Vesta-like asteroids in the early history of the solar system.

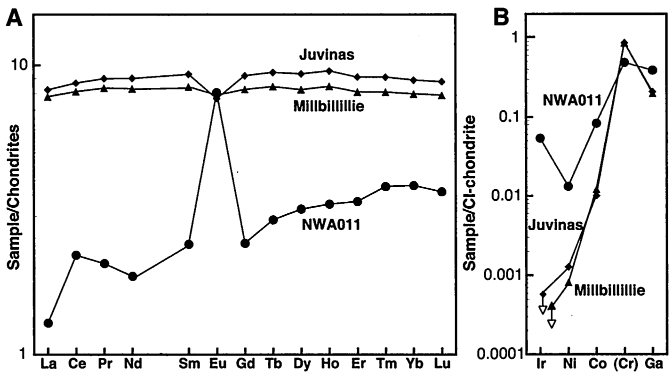

Fig. 2. (**A**) Chondrite-normalized rare earth element patterns of NWA011, and eucrites, Juvinas and Millbillillie. (**B**) CI-chondrite–normalized siderophile element abundances of NWA011, Juvinas, and Millbillillie. The chondrite and CI abundances for normalization are from (*34*) and (*17*), respectively.

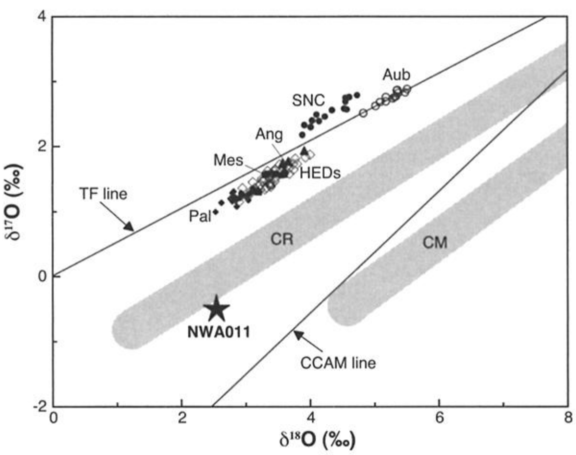

Fig. 3. Oxygen isotopic compositions of NWA011 and other meteorites (*22*). HEDs, a class of differentiated meteorites (howardite, eucrite, and diogenite); Ang; angrites, Mes; silicate inclusions in mesosiderites, Pal; pallasites, SNC; martian meteorites, Aub; aubrites; CR and CM; carbonaceous chondrites, TF line; terrestrial fractionation line, CCAM line, carbonaceous chondrite anhydrous mineral line.

References and Notes

1. J. T. Wasson, G. W. Wetherill, in *Asteroids*, T. Gehrels, Ed. (Univ. of Arizona Press, Tucson, AZ, 1979), pp. 926–974.
2. D. W. Mittlefehldt, T. J. McCoy, C. A. Goodrich, A. Kracher, in *Planetary Materials, Reviews in Mineralogy*, vol. 36, chap. 4, J. J. Papike, Ed. (Mineralogical Society of America, Washington, DC), pp. 1–195.
3. Only three groups of basaltic meteorites with asteroidal origin (eucrites, angrites, and basaltic inclusions of mesosiderites) have been sampled to date. The basaltic inclusions in mesosiderites are mineralogically similar to eucrites, but the genetic relationships between the two basalts have been yet controversial. Angrites are a small group of basaltic meteorites, mineralogically different from eucrites. The oxygen isotopic compositions of these basaltic meteorites indicate derivation from a common isotopic reservoir (*23*). In contrast to the strong link between eucrite and 4 Vesta, the parent bodies of angrites and mesosiderites remain unidentified. See (*2*) for detail.
4. R. P. Binzel, S. Xu, *Science* **260**, 186 (1993).
5. S. V. Afanasiev, M. A. Ivanova, A. V. Korochantsev, N. N. Kononkova, M. A. Nazarov, *Meteor. Planet. Sci.* **35**, A19 (2000).
6. NWA011 was found in the Sahara desert with total known mass of 40 g, and was initially classified as a eucrite (*5*). A broken surface of NWA011 shows a rusty appearance due to the presence of weathering products. Polished thin and thick sections of NWA011 were examined by optical and scanning electron microscopy and by electron microprobe. A portion of the sample weighing ~1.5 g was powdered for standard wet chemical analysis, instrumental neutron activation analysis (INAA) including prompt gamma-ray analysis (PGA), and inductively coupled

plasma–mass spectrometry (ICP-MS). Other portions were used for noble gas and oxygen isotopic analysis. The analytical procedures were described in (*27–32*). Note that two oxygen isotopic analyses were performed with and without HCl wash to remove weathering products, and the two results are the same. This indicates that the oxygen isotopic composition of NWA011 was not changed during the weathering processes in the desert. This result is consistent with the very low Fe_2O_3 contents determined by wet chemical analysis (*7*).
7. Supplementary material is available on *Science* Online at www.sciencemag.org/cgi/content/full/296/5566/334/DC1
8. A. Yamaguchi *et al.*, *Geochim. Cosmochim. Acta* **65**, 3577 (2001).
9. H. Takeda, A. L. Graham, *Meteoritics* **26**, 129 (1991).
10. A. Yamaguchi, G. J. Taylor, K. Keil, *Icarus* **124**, 97 (1996).
11. R. Kretz, *Geochim. Cosmochim. Acta* **46**, 411 (1982).
12. Y. Ikeda, H. Takeda, *Proc. Lunar Planet. Sci. Conf.* **15**, C649 (1985).
13. A. El Goresy, P. Ramdohr, *Proc. Lunar Sci. Conf.* **6**, 729 (1975).
14. C. Floss, G. Crozaz, A. Yamaguchi, K. Keil, *Antarct. Meteorite Res.* **13**, 222 (2000).
15. M. Miyamoto, M. B. Duke, D. S. McKay, *Proc. Lunar Planet. Sci. Conf.* **15**, C629 (1985).
16. B. Mason, E. Jarosewich, J. A. Nelen, *Smithson. Contrib. Earth Sci.* **22**, 27 (1979).
17. E. Anders, N. Grevesse, *Geochim. Cosmochim. Acta* **53**, 197 (1989).
18. J. Willis, J. I. Goldstein, *Proc. Lunar Planet. Sci. Conf.* **13**, *J. Geophys. Res.* **87**, A435 (1982).
19. The isotopic compositions of He, Ne and Ar represent the predominance of cosmogenic components and radiogenic ^{40}Ar (*7*). Heavy noble gases, Kr and Xe, are composed of trapped (probably adsorbed terrestrial atmospheric gas), cosmogenic and fission components. The cosmic-ray exposure ages, determined from cosmogenic ^{3}He, ^{21}Ne and ^{38}Ar, are 11, 30, and 23 Ma, respectively. The shorter ages from ^{3}He and ^{38}Ar are probably due to partial loss of these gases by terrestrial weathering (*33*). The ^{81}Kr-Kr age for NWA011 is 39 ± 5 Ma, which can be interpreted as an upper limit of the cosmic-ray exposure age (*7*). Abundance of radiogenic ^{4}He is very low ($<1 \times 10^{-7}$ cm^3/g), and the measured $^{3}He/^{4}He$ ratio is purely cosmogenic. From this amount and the bulk U content for NWA011 (*7*), the U-^{4}He age can be constrained as <0.03 billion years (Ga). Radiogenic ^{4}He may have been lost during atmospheric entry to the earth or by terrestrial weathering.
20. O. Eugster, Th. Michel, *Geochim. Cosmochim. Acta* **59**, 177 (1995).
21. Oxygen isotopic compositions are expressed as delta-values, the deviation in per mil relative to a standard composition (standard mean ocean water, or SMOW) $\delta^{18}O = \{[(^{18}O/^{16}O)_{sample}/(^{18}O/^{16}O)_{SMOW}] - 1\} \times 1000$ (‰) and similarly for $\delta^{17}O$. The deviation of the oxygen isotopic composition from the terrestrial fractionation line is expressed by $\Delta^{17}O$, where $\Delta^{17}O = \delta^{17}O - 0.52\delta^{18}O$.
22. R. N. Clayton, *Annu. Rev. Earth Planet. Sci.* **21**, 115 (1993).
23. R. N. Clayton, T. K. Mayeda, *Geochim. Cosmochim. Acta* **60**, 1999 (1996).
24. A. Yamaguchi, G. J. Taylor, K. Keil, *J. Geophys. Res.* **102**, 13381 (1997).
25. T. Hiroi, unpublished data.
26. D. Lazzaro *et al.*, *Science* **288**, 2033 (2000).
27. H. Haramura, I. Kushiro, K. Yanai, *Mem. Natl. Inst. Polar Res., Spec. Issue* **30**, 109 (1983).
28. K. Shinotsuka, M. Ebihara, *Anal. Chim. Acta* **338**, 237 (1997).
29. S. A. Latif *et al.*, *J. Radioanal. Nucl. Chem.* **239**, 577 (1999).
30. M. Ebihara, T. Miura, *Geochim. Cosmochim. Acta* **60**, 5133 (1996).
31. R. N. Clayton, T. K. Mayeda, *Earth Planet. Sci. Lett.* **62**, 2 (1983).
32. Y. N. Miura, K. Nagao, N. Sugiura, T. Fujitani, P. H. Warren, *Geochim. Cosmochim. Acta* **62**, 2369 (1998).
33. E. K. Gibson Jr., D. D. Bogard, *Meteoritics* **13**, 277 (1978).
34. M. Ebihara, unpublished data.
35. We thank K. Shiraishi, H. Takeda, T. Hiroi, K. Keil, and T. Mikouchi for discussion, K. Hayano for technical assistance, and the Musée National D'Histoire Naturelle (Paris) for providing the sample of Juvinas. We acknowledge support by Grants-in-Aid for Scientific Research from the Ministry of Education, Science, Culture, Sports, Science and Technology, Japan, Nos. 12740300 (A.Y.), 1144017 (M.E.), and 11640487 (K.N.), and NSF grant EAR9815338 (R.N.C.).

27 December 2001; accepted 6 March 2002

African Pastoralism: Genetic Imprints of Origins and Migrations

Olivier Hanotte,[1]* Daniel G. Bradley,[2] Joel W. Ochieng,[1] Yasmin Verjee,[1] Emmeline W. Hill,[2] J. Edward O. Rege[3]

The genetic history of African cattle pastoralism is controversial and poorly understood. We reveal the genetic signatures of its origins, secondary movements, and differentiation through the study of 15 microsatellite loci in 50 indigenous cattle breeds spanning the present cattle distribution in Africa. The earliest cattle originated within the African continent, but Near East and European genetic influences are also identified. The initial expansion of African *Bos taurus* was likely from a single region of origin. It reached the southern part of the continent by following an eastern route rather than a western one. The *B. indicus* genetic influence shows a major entry point through the Horn and the East Coast of Africa and two modes of introgression into the continent.

Cattle pastoralism is widespread in Africa today and still forms the basis of life for millions across the continent. Two hypotheses for the origins of African domesticated cattle are currently debated. The North African subspecies of wild cattle or aurochs *Bos primigenius* (*1*) may have undergone an indigenous African domestication around 10,000 years ago, possibly in the northeast of the continent (*2–4*). However, the archaeological evidence is disputed and the molecular data are not conclusive (*2*, *5*). Alternatively, domesticated cattle could have been introduced into Africa from the Near East where cattle domestication is known to have occurred (*6*).

The pattern and the chronology of subsequent domestic cattle dispersal within the continent are also unclear. The origin and history of the early dispersion of African pastoralism westward and southward in the continent remain largely unknown, as does the pattern of the introgression of *B. indicus*, which is known to have influenced the majority of cattle populations in Africa (*7*, *8*).

Pictorial representations and archaeological remains show that the earliest African cattle were humpless *B. taurus* (*9*, *10*). The earliest evidence for humped cattle on the continent, provided by Egyptian tomb paintings of the XIIth Dynasty, do not appear until the second millennium BC (*11*, *12*), which suggests that the Egyptian civilization may have played a role in the introduction of zebu into the continent. Today, most modern breeds have an appreciable zebu ancestry (*7*, *8*), which attests to a major secondary introduction.

We address these issues through a continent-wide sampling of indigenous African cattle. Fifty populations from 23 African countries spanning the present cattle distribution in Africa (*13–15*) were studied (Fig. 1A). The sample included 31 *B. taurus* (taurine) populations, generally found in more tropical regions in West, East, and Southern Africa, and 19 *B. indicus* (zebu) populations, restricted to the more arid zones of West and East Africa (*11*, *13*).

These samples were analyzed with 15 autosomal microsatellite markers (*14*). We observed 183 alleles whose frequencies were used to calculate the principal components (PC) values of the genetic variation (*14*). PC values of each population were then used to construct interpolation maps illustrating continent-wide genetic trends for the first three PCs (Fig. 1, B through D) (*16*). These allowed us to generate hypotheses, which were assessed statistically and in light of earlier mitochondrial and Y chromosome DNA results (*4*, *8*, *17*), as well as available archaeological and historic information.

The first principal component of the vari-

[1]International Livestock Research Institute, Post Office Box 30709, Nairobi, Kenya, [2]Department of Genetics, Smurfit Institute, Trinity College, Dublin 2, Ireland. [3]International Livestock Research Institute, Post Office Box 5689, Addis Ababa, Ethiopia.

*To whom correspondence should be addressed. E-mail: o.hanotte@cgiar.org